inter.noise
HAMBURG 2016

Scattering from objects and surfaces in room acoustical simulations

Gerd MARBJERG[1, 2], Jonas BRUNSKOG[2], Cheol-Ho JEONG[2], Erling NILSSON[1]
[1]Saint-Gobain Ecophon, Hyllinge, Sweden
[2]Acoustic Technology, Department of Electrical Engineering
Technical University of Denmark, Kgs. Lyngby, Denmark

ABSTRACT

In room acoustical simulations, scattering objects are often modeled as impenetrable boxes with high scattering coefficients assigned to the surfaces. In some cases, a cluster of objects is modeled as a virtual impenetrable box, such that no sound propagation can take place between the objects. Thus, the scattering only takes place on the boundary surfaces of the box and the acoustic volume of the room is reduced. Another challenge with representing scattering objects by reflecting surfaces is that it increases the number of surfaces, which greatly increases the calculation complexity for methods such as the image source method. In this paper a modeling method where the scattering from objects takes place in certain parts of the room volume is proposed. In this method, sound can still travel through scattering objects, but be partly scattered. This volume scattering method has at present been implemented in the simulation tool PARISM (Phased Acoustical Radiosity and Image Source Method). Scattering from objects and surfaces is likely to be strongly frequency dependent and the frequency dependence can depend on their sizes, shapes and structure. The importance of the frequency dependence is investigated and discussed through simulations.

Keywords: Sound scattering, geometrical acoustics. I-INCE Classification of Subjects Number: 76.9

1. INTRODUCTION

In a room, sound is scattered due to objects and surface irregularities. This scattering is of high importance for the resulting sound field, especially for shoebox-shaped rooms like most classrooms and offices, and the modeling of scattering should therefore be given some consideration when simulating the sound field in a room. In geometrical room acoustics, it is often assumed that all scattering takes place on the surfaces. Much work has been done on surface scattering and how it should be considered in room acoustic simulations [1–3]. Less attention has however been given to how scattering from objects in the volume should be modeled. Guidelines might be given for how to model the scattering objects, such as it is the case in the manual for the well-established tool ODEON [4]. In practice, boxes are often drawn to represent single or clusters of scattering objects and high surface scattering coefficients are assigned to the surfaces of these boxes. With this approach, the boxes are impenetrable and the acoustic volume of the room is thus reduced. This method furthermore introduces many more surfaces from which reflections must be considered. For a simulation method, such as the image source method, this greatly increases the calculation complexity.

Some work has been done to model the influence of scattering objects on the sound levels in industrial spaces [5–9], but these methods only describe the attenuation due to the scattering and are furthermore not easily implemented in geometrical acoustic models. Attenuation due to scattering in parts of a volume has been implemented in the image source method by Dance and Shield [10], but the contribution of scattered sound energy to the sound field was not taken into account. In the present work it is therefore proposed to regard the scattering from objects as something that takes place in part of a room volume and that attenuates specularly reflected energy and contributes to diffusely reflected energy.

The concept of volume scattering is known from other fields of acoustics, e.g. in outdoor sound propagation and underwater acoustics. A bulk scattering coefficient can be defined for a volume within which sound is scattered during propagation. The scattering can be due to a single object, a collection of objects

[2]email: jbr@elektro.dtu.dk

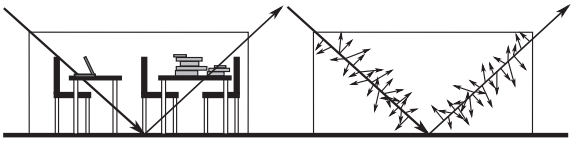

Figure 1: Sketch of volume with scattering objects and the equivalent enclosing volume, and how the scattering is assued to take place homogeneously within this volume.

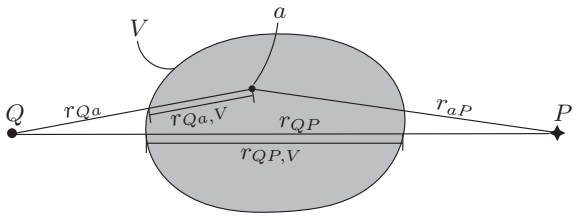

Figure 2: Sketch of a scattering volume V in free space through which sound passes from the source Q and is received at the receiver P.

or fluctuations in the physical properties of the volume. The bulk scattering coefficient is defined as the loss of intensity per unit length by an incident plane wave due to scattering divided by the intensity of the incident wave [11]. Different notations and definitions are used in references from different fields. Here, the definitions of Morfey [11] are used, but with a different notation. In some fields, the scattering cross section is used rather than the bulk scattering coefficient. The bulk scattering coefficient is defined as the scattering cross section per unit volume. In the present work, the bulk scattering coefficient and the differential bulk scattering coefficient are preferred. The differential bulk scattering coefficient is defined as the bulk scattering coefficient per unit solid angle and thus as the scattering cross section per unit volume per unit solid angle. A penetrable volume enclosing a cluster of objects is introduced in a room, and within this volume, the objects are randomly positioned, and it is thus assumed that the scattering takes place homogeneously and uniformly such that an angle-independent bulk scattering can be assigned to the volume of the box. An illustration of this can be seen in Fig. 1, where an example of tables with chairs and objects is shown. In practice, the precise locations of such objects are rarely known. This is for instance true for a classroom where students are expected to move the tables and chairs around slightly. It is therefore convenient to define a volume within which the objects are assumed to be located without knowing their exact locations, and thus statistically modeling an average of all possible configurations.

The volume scattering is implemented in the room acoustic model PARISM [12], which is a phased combination of acoustical radiosity (AR) with the image source method (ISM). This model includes angle-dependent and phased boundary conditions. When using angle-dependent boundary conditions, scattering is of particularly high importance, as scattering has a great influence on the angle of incidence of sound on a surface. PARISM has been developed with particular focus on rooms with porous absorber ceilings of which the sound absorbing properties often are highly angle-dependent and scattering therefore has to be handled with care in PARISM. PARISM is an extension of CARSIM [13] that is an energy-based combination of the image source method and acoustical radiosity where the phase and angle dependence of reflections are disregarded.

This paper contains the basic equation of the volume scattering method. It furthermore shows examples of results from geometrical modelling with scattering from furniture and surface roughness.

2. SCATTERING FROM A VOLUME IN FREE SPACE

A volume V that homogeneously and uniformly scatters sound with a bulk scattering coefficient of s'_v is placed in free space. It has only convex angles seen from outside the volume as sketched in Fig. 2. The point source Q has the power Π_Q equally distributed in all directions and emits sound waves which are assumed to be plane when passing through the volume. The total sound energy density at P is the sum of the direct

contribution from the source and a scattered contribution, so

$$w(P,t) = w_{dir}(P,t) + w_{scat}(P,t). \tag{1}$$

The bulk scattering coefficient is defined as the loss of intensity by an incident plane wave due to scattering divided by the intensity of the incident wave [11], which means that the direct contribution from Q to P is

$$w_{dir}(P,t) = \frac{\Pi_Q(t - r_{QP}/c)}{\rho\, c^2\, r_{QP}^2}\, \mathrm{e}^{-s'_v \cdot r_{QP,V}}, \tag{2}$$

where s'_v is the bulk scattering coefficient, r_{QP} is the distance between the source and the receiver and $r_{QP,V}$ is the distance traveled in V between the source and the receiver, see Fig. 2.

A first approximation is that only first order scattering is considered and that the scattering is assumed to be weak. Weak scattering means that the incident sound field at any point in the scattering volume can described by the incidence field in the absence of the scattering volume. The case is first regarded in steady state and the scattered sound energy density from volume V can then be found by an integration over V as [14, 15]

$$w_{scat}(P) = \int_V w_0(a) \frac{\Delta s'_v(\theta)}{r_{aP}^2}\, dV, \tag{3}$$

where a is the integration point in V, $w_0(a)$ is the incident undisturbed field from the source in a, $\Delta s'_v(\theta)$ is the differential bulk scattering coefficient, and r_{aP} is the distance between a and the receiver P, see Fig. 2. From the differential bulk scattering coefficient, the bulk scattering coefficient can be found by solid angle integration over all directions [11]. Because it is assumed that the scattering is uniform and homogeneous and thus angle-independent, the relation between s'_v and $\Delta s'_v(\theta)$ can be simplified to $s'_v = 4\pi\, \Delta s'_v(\theta)$. If the scattering is no longer regarded in steady state, the time delay between the integration point a and the receiver P must be considered for each point. Including this and assuming homogeneous and uniform scattering in Eq. (3) gives

$$w_{scat}(P,t) = \int_V w_0(a, t - r_{aP}/c) \frac{s'_v}{4\pi\, r_{aP}^2}\, dV. \tag{4}$$

In the present case, it is of interest to allow for scattering that is not very weak. The attenuation of the incident field in point a due to the scattering on the traveled path through V before reaching a is therefore included. Inserting the expression for the incoming sound energy density from Eq. (2) thus gives

$$w_{scat}(P,t) = \int_V \frac{\Pi_Q(t - (r_{Qa} + r_{aP})/c)}{\rho\, c^2\, r_{Qa}^2} \frac{s'_v}{4\pi\, r_{aP}^2}\, \mathrm{e}^{-s'_v \cdot r_{Qa,V}}\, dV, \tag{5}$$

where r_{Qa} is the distance between Q and the integration point a, and $r_{Qa,V}$ is the distance traveled through V between the source Q and the integration point a, see Fig. 2.

To simplify the implementation of Eq. (5), the volume V is discretized into N_n small elements. Assuming that the energy density is constant within each of the volume elements gives the following expression

$$w_{scat}(P,t) = \sum_{n=1}^{N_n} \frac{\Pi_Q(t - (r_{Qn} + r_{nP})/c)}{\rho\, c^2\, r_{Qn}^2} \frac{s'_v}{4\pi\, r_{nP}^2}\, \mathrm{e}^{-s'_v \cdot r_{Qn,V}}\, V_n, \tag{6}$$

where r_{Qn} is the distance between Q and a central point in the volume element n, r_{nP} is the distance between n and the receiver P, V_n is the volume of n, and $r_{Qn,V}$ is the distance traveled in V between Q and n.

2.1 Reflecting surface and scattering volume in free space

A reflecting surface S_r is introduced in the presence of the point source and the volume V. It is assumed to be totally reflecting such that it causes no energy loss. The reflection from the surface is included by creating an image source q of the source Q. Higher order scattering between volume elements is disregarded. Sound that is scattered by V can however subsequently be reflected by S_r, and this reflected sound can afterward again be scattered and then again be reflected and so on. Since no absorption is included in the present example, the process of scattering followed by reflection will in theory continue infinitely. The equivalent is true for sound which is first reflected by S_r and then scattered by V. A decision must therefore be made about how

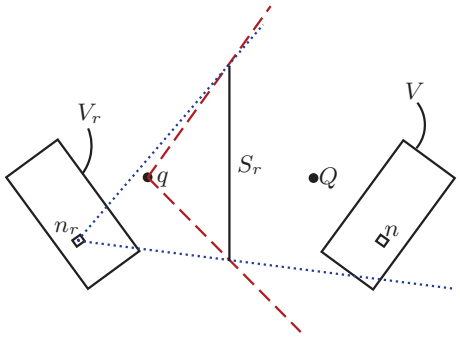

Figure 3: 2D illustration of the field angles of the image source q (red dashed lines) and the image element n' (blue dotted lines).

high orders of reflection and scattering are considered. Here, it is chosen that only first order scattering to reflection and reflection to scattering should be included. This gives five separate contributions to the receiver. For each of these contributions it must be considered whether they are attenuated by V and whether they are obstructed by S_r. The contributions are the following:

1. The direct contribution from Q that is found by Eq. (6) and that can be both attenuated by V and obstructed by S_r.

2. The scattered contribution from Q that is found by Eq. (2). This can also be obstructed by S_r.

3. The contribution from q, which is valid within the field angle of q as illustrated in Fig. 3 by the red dashed lines. The contribution can furthermore be attenuated by V. This contribution is found by Eq. (6) with $Q = q$.

4. The contribution that has first been reflected by S_r and then scattered by V. This is seen as a scattered contribution from q. This contribution is only valid for volume elements within the field angle of q. In Fig. 3, this is true for all elements. If higher order reflection and scattering is considered, the contributions to some receivers from some volume elements are obstructed by S_r like the scattered contributions from Q. This obstruction is however disregarded here due to the limited reflection order. The contribution can be found by

$$w_{scat,q}(P,t) = \sum_{n=1}^{N_n} \frac{\Pi_Q(t-(r_{qn}+r_{nP})/c)}{\rho\, c^2\, r_{qn}^2} \frac{s'_v}{4\pi\, r_{nP}^2}\, \mathrm{e}^{-s'_v \cdot r_{Qn,V}}\, V_n. \tag{7}$$

5. The contribution which has first been scattered by V and then been reflected by S_r. This is seen as a contribution from an image volume, V_r of V. See Fig. 3 for an illustration. For this contribution, the field angles of the volume elements should be considered. This is illustrated in Fig. 3 by the blue dotted lines for the image volume element n_r. The possible attenuation by V should be considered if higher order scattering was considered. This attenuated is disregarded here due to the limited scattering order. The contribution can be found by the following expression.

$$w_{scat,V_r}(P,t) = \sum_{n=1}^{N_n} \frac{\Pi_Q(t-(r_{Qn}+r_{n_rP})/c)}{\rho\, c^2\, r_{Qn}^2} \frac{s'_v}{4\pi\, r_{n_rP}^2}\, \mathrm{e}^{-s'_v\, r_{Qn,V}}\, V_n \tag{8}$$

In the above case higher order scattering and reflection is not permitted in order to keep down the calculation complexity. A further simplification of the case could be to only allow specular to scattered reflection. That means that the sound from the source and the image source can be scattered once, but sound that has once been scattered cannot afterward be specularly reflected. This approximation can be a practical one when a scattering volume is placed in a room and several reflecting surfaces must be considered, because creating image volumes is computationally heavy. In this case only the first four contributions should be considered and the scattered contribution from Q (the 2nd on the list) cannot be obstructed by S_r.

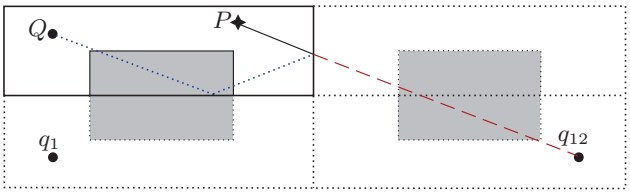

Figure 4. Imaging of a room with a scattering volume.

2.2 Summary of Sec. 2

The basic equations of the volume scattering method have been outlined. Validation of these equations in terms of energy conservation can be found in future work by the authors [16]. It has furthermore been shown how a reflecting surface in the presence of the volume can be handled, which is a good first step for introducing the scattering volume in geometrical room acoustic simulations.

3. SCATTERING VOLUME IN PARISM

The volume scattering method is implemented in the room acoustic model PARISM (Phased Acoustical Radiosity and the Image Source Method) [12]. This model uses the image source model (ISM) for specular reflections and acoustical radiosity (AR) for the diffuse reflections. In AR, the surfaces are divided into elements that diffusely exchange radiation according to Lambert's law. Radiation density is defined as the rate at which sound energy leaves a unit surface area [17]. This paper only outlines how the volume scattering method can be included in PARISM. For more details about the implementation the authors refer to upcoming work [16].

For the implementation of a scattering volume in PARISM, it should be decided how to apply Eqs. (2) and (6). In Eq. (2) there is an attenuation of the direct contribution due to the scattering volume, and in Eq. (6) there is a contribution from the scattering volume. These equations should be implemented such that the energy is conserved and the attenuation should thus correspond to the scattered contribution. It is natural to consider the image sources in ISM as radiating towards the scattering volume and thus as sources in Eq. (6). When they are considered as sources in Eq. (6), their direct contributions to the receiver and the AR elements should be equally attenuated as described by Eq. (2). The scattered contributions from the image sources should then be sent to the receiver and the AR elements like the direct contributions. The AR elements are also seen as sources in Eqs. (2) and (6), but this is a computationally heavy task because all surface elements will have to be considered for all volume elements. An approximation of this is therefore used, which will be available in reference [16].

In Sec. 2.1, equations were given for the case of a single reflecting surface in the presence of a scattering volume. It was mentioned that this can be modelled both with and without allowing scattered to specular reflection. The calculation complexity greatly increases by including scattered to specular reflection because an image of the scattering volume must be considered. If this should be done for a room, an image of the volume should be created for each surface and each reflection order. This is illustrated in Fig. 4, where a room with a rectangular scattering volume is shown along with images of the volume and source. As it would be a very computationally heavy task to determine the contributions from all elements in the image volumes, it is not included in the present implementation to PARISM, and sound that has been scattered by a volume can therefore only be diffusely reflected in AR.

4. MODELING SCATTERING IN ANOTHER GEOMETRICAL ROOM ACOUSTIC SIMULATION TOOL

The well-established room acoustical simulation tool ODEON is used for comparison with PARISM simulations. ODEON is a hybrid tool, combining the image source for early reflections with ray tracing for later reflections [4]. Angle-independent absorption coefficients are used as input in ODEON, but for soft surfaces ODEON can apply a standard curve of the angle dependence. This curve is based on locally reacting materials and is thus an approximation, but it does consider the fact that the absorption coefficients of absorbers

are often low at high angles of incidence and can therefore improve the results compared to not including any angle-dependence.

The modeling of scattering in ODEON is vector-based and the resulting reflected ray is calculated by weighting the specular direction and a random scattered direction by means of the scattering coefficient. The random scattered direction is found by a method of oblique Lambert [4]. Only a single value scattering coefficient can be set for each surface in ODEON. The frequency dependence thus cannot be chosen freely, but will follow a predefined curve. Examples of such curves can be found in the manual of ODEON [4].

ODEON has reflection based scattering implemented, which considers the size of a surface, the angle of incidence and the frequency to calculate the resulting scattering. Further details on the subject can be found in the work by Zeng et al. [18]. Scattering due to limited size of surfaces in PARISM should be included in the set scattering coefficients and thus cannot at the present stage of PARISM depend on the angle of incidence of and distance to a specific reflection. It would however be possible to include reflection based scattering in PARISM because angles of reflections are already determined for the absorption properties.

Scattering from objects in ODEON must be applied to surfaces. According to the manual, an audience should be modeled as a box of 0.7 m height with appropriate scattering and absorption coefficients assigned. The recommendations for modeling furniture are less specific and depend on whether the objects are expected to create strong early reflections. If this is not expected the only recommendation is to include the scattering and absorption in the region where it is present [4]. Only a single value scattering coefficient can be set for each surface in ODEON. The frequency dependence thus cannot be chosen freely, but will follow a predefined curve. Examples of such curves can be found in the manual of ODEON [4], where the it is recommended to set the scattering coefficient equal to that of a mid-frequency value, and the mean of the 500 Hz and 1 kHz octave bands is a suggested choice.

In ODEON, it is possible to make a surface semi-transparent with a given transparency. The manual recommends to do this if many small surfaces are to be modeled by a single large one. This function will be tested in comparison between a semi-transparent scattering box in ODEON and a scattering volume in PARISM.

5. EXAMPLES

In this section, two examples of rooms with scattering are investigated with measurements and with PARISM and ODOEN simulations. The first example is a room with and without furniture and the second is a scale model box with and without a sinusoidal diffuser on the wall. Both object and surface scattering are thus investigated.

5.1 Furnished room

The dimensions of the room are [7.32 x 7.57 x 2.7] m with its center positioned in (3.66, 2.785, 1.35), and it has a suspended porous absorber ceiling. 2.7 m is the height up to the ceiling surface. The ceiling is 5 cm thick, has a flow resistivity of 12 $\frac{\text{kPa s}}{\text{m}^2}$ and the air gap is 75 cm. The impedance of the ceiling is calculated using Miki's model [19]. The absorption coefficients of the walls and floor are estimated from reverberation time measurements in the empty room without an absorbing ceiling. It is assumed that the sound field in the room is then diffuse enough to apply Sabine's law to determine an average absorption coefficient, α_{av}, which is shown in Table 1. The surface scattering coefficients are not known, but are set very low as they meant to represent surfaces with no more irregularities than windows and doors. The values have then been optimized for the PARISM simulation of the unfurnished room to fit the measurements and are denoted s in Table 1. The source is placed in (3.69, 6.45, 1.5) and the receiver is placed in (1.51, 3.88, 1.2).

The measurements have been done at the laboratories at Ecophon in Hyllinge, Sweden with equipment from Brüel & Kjær. The measurements were done with and without furniture that consisted of 9 tables with 18 lightly upholstered chairs, similar to the furnishing found in a small classroom, see left side of Fig. 5.

5.1.1 Method of the PARISM simulations

For this example the volume scattering method is used. Two rectangular scattering volumes are tested in the simulations: the first, V_1, has dimensions [4.7 x 3.52 x 1] m and its center in (3.65, 3.24, 0.5) and the second, V_2, has dimensions [4.7 x 3.52 x 1.5] m and its center in (3.65, 3.24, 0.75). Both volumes enclose

Table 1. The input data for the simulations of the room with furniture.

f_c[Hz]	63	125	250	500	1000	2000	4000
α_{av}	0.075	0.057	0.046	0.035	0.036	0.047	0.050
α_{ceil}	0.80	0.75	0.72	0.70	0.73	0.83	0.86
s	0.03	0.04	0.06	0.065	0.05	0.05	0.035
s'_{v1} [m^{-1}]	0	0	0.255	0.542	0.697	0.799	0.881
s'_{v2} [m^{-1}]	0	0	0.170	0.361	0.464	0.533	0.587
s_{furn}	0	0	0.49	0.76	0.84	0.88	0.91
α_{furn}	0.07	0.07	0.285	0.315	0.35	0.36	0.35
m'_{v1} [m^{-1}]	0.027	0.027	0.123	0.142	0.161	0.167	0.161
m'_{v2} [m^{-1}]	0.018	0.018	0.084	0.094	0.107	0.111	0.107

Figure 5: **Left:** The furnished room of the first example. **Right:** The scale model of the second example with the sinusoidal diffuser.

the furnishing of the measurements. The bulk scattering of volume V_2 is such that $s'_{v2} = s'_{v1}\,V_1/V_2$, which means that the total scattering cross section of the two volumes are equal. The big difference between the two volumes is that the height of V_1 is below the height of both the source and the receiver, but the height of V_2 is above the receiver and at the same height as the source. For V_2 that will mean that the direct contribution from the source and the contributions from any image sources at the same height as the source will be intercepted by V_2. The scattering cross sections of the volumes have been estimated by use of the model of diffraction from edges by Svensson et al. [20–22]. From this model, it is possible to calculate the scattering cross section of a single polygon or a collection of polygons. Here, the total scattering cross is found as the sum the scattering cross sections of 9 rectangles of dimensions [1.2 x 0.6 x 0.05] m representing the table tops and 36 rectangles of dimensions [0.5 x 0.4 x 0.05] m representing the seats and backs of the chairs. The bulk scattering coefficient can then be found by dividing the scattering cross section by a volume that encloses the volume and the choice of this volume is what differs for V_1 and V_2. When the decay curves of the measurements were regarded, it was noticed that the furniture did not seem to have any influence on the 63 and 125 Hz octave bands and the bulk scattering coefficients at these frequencies were therefore assumed to equal zero.

To get a better correlation with measurements, absorption has been added to the scattering volume. This is done by adding the bulk absorption coefficient m'_v to s'_v in all places where s'_v is used to account for attenuation due to scattering, thus in all equations where it is in an exponential. Since no data for bulk absorption coefficients were available, they have been estimated from measured absorption coefficients which are more easily available. The surface absorption coefficients of the tables are estimated based on data for a wooden door and the surface absorption coefficients of the chairs are estimated based on measurements of unoccupied chairs [23]. No data was available for 63 Hz octave band, so these are set equal to those of the 125 Hz band. Due to the lack of influence of the furniture on the measurements, the absorption coefficient of the chairs were assumed to equal zero at 63 and 125 Hz, such that the average surface absorption coefficient is as can be seen in Table 1 denoted α_{furn}. The surface scattering coefficients are determined with the assumption that sound is absorbed when it hits the surface where the objects are placed. For the scattering volume it is assumed that this corresponds to the sound entering the volume, traveling the through the volume, being reflected by the floor and then again traveling through the volume before exciting. On average the sound travels the distance of the mean free path before and after reflection. It should therefore be true that $(1-\alpha_{furn}) = \mathrm{e}^{-2\,m'_v\,\bar{r}_V}$. m'_v can thus be found by $m'_v = -\ln(1-\alpha_{furn})/(2\,\bar{r}_V)$, which gives the unit m^{-1} for the bulk absorption coefficient as it should. The bulk absorption coefficients for V_1 and V_2 can be

seen in Table 1 denoted m'_{v1} and m'_{v2}, respectively.

5.1.2 Method of the ODEON simulations

In ODEON, all surfaces must have assigned an angle-independent absorption coefficient. Paris' law is therefore used to determine a random incidence scattering coefficient from the reflection factor that is used in PARISM. The random incidence absorption coefficient is denoted α_{ceil} in Table 1.

The furniture is modeled by a box in the same positions as the ones in PARISM, but it has been chosen to make it 0.7 m in height. This is done because a such a box in ODEON will cause reflections from the surfaces and no surfaces should therefore be closer to the receiver than they were in the measurements. Two ODEON simulations are done: one where the box is impenetrable and one where the surfaces are semi-transparent with a transparency of 0.5. The scattering coefficient of the surfaces of the box has been estimated from the bulk scattering coefficient of the volume in PARISM by the inverse considerations as were used to estimate the bulk absorption coefficient of the volume. It is thus assumed that $(1-\alpha_{furn})(1-s_{furn}) = \mathrm{e}^{-s'_v\, 2\,\bar{r}_V}$, which means that $s_{furn} = 1 - \mathrm{e}^{-s'_v\, 2\,\bar{r}_V}/(1-\alpha_{furn})$. The resulting scattering coefficient can be seen in Table 1, but as mentioned in Sec. 4 ODEON needs only the mid-frequency value as input, and 0.4 chosen for that.

5.2 Scale model with sinusoidal diffuser

The scale model is a wooden box of dimensions [1.57 x 1.25 x 1] m, and is thus seen as a 1:5 scale model of a classroom, although this does correspond to a very high ceiling height. It might be more realistic as a 1:3 scale model of a small office. Regardless, no rescaling is done as the simulations are done with the same dimensions too avoid errors in such processing. The frequency range of interest is however scaled compared to what is normally regarded in room acoustics and thus includes the 250 Hz octave band to the 16 kHz octave band. The sampling frequency of the measurements and of the PARISM simulations is 48 kHz. For the ODEON simulations, it was not possible to change the frequency range, and the 250 Hz to 8 kHz octave bands therefore limit the comparison with the ODEON simulations.

As for the first example, the absorption coefficients α_{av} of the walls and the floor are estimated from reverberation time measurements in the empty box without an absorbing ceiling, see Table 2. The box has been fitted with a porous absorber ceiling of 15 mm thickness with an 85 mm air gap behind it, see right side of Fig. 5, which gives a resulting height of 0.9 m. The impedance is calculated using Miki's model [19]. The random incidence absorption coefficient of the ceiling is denoted α_{ceil} and is seen in Table 2.

A sinusoidal diffuser is introduced in the box, which is 3 cm thick and round with a diameter of 80 cm, which gives an area of 0.5 m^2. The period of the diffusing pattern is 10 cm. The measurements were done with two orientations: vertical and horizontal, and in right side of Fig. 5 the sinusoidal diffuser is seen in the scale model in the vertical orientation. The scattering coefficient of the diffuser has been measured following ISO standard 17497-1 [24], thus under assumed diffuse field conditions and the values can be found in Table 2 denoted s_{sin}. The Sabine absorption coefficient of the sinusoidal scatterer has been measured following ISO standard 354 [25], but unfortunately no information about the angle-dependence of or phase shifts on reflections from the diffuser was available. The absorption coefficient is denoted α_{sin} and is give in Table 2.

The measurements were done with a Vifa (XT25TG30-04) tweeter loudspeaker placed in a corner of the box pointing towards the diagonally opposite corner. In standard measurements, an omnidirectional source should be used, but no omnidirectional source, which was suitable for the scale model, was available. The directivity of the loudspeaker has been measured, which can be used for the simulations.

5.2.1 Method of the PARISM simulations

The scattering coefficients of the ceiling and the floor are set to 0.01 for all frequencies. For the walls, it was initially set to 0.04 for all frequency bands for and the frequency dependence was then altered such that the simulated decay curves fit the measured ones best possible. The resulting scattering coefficients can be seen as s_w in Table 1.

In the simulations, all surfaces must be defined as polygons and though it is possible to approximate a circle by several polygons, it has been chosen to represent the scatterer as a square. A square of surface area 0.5 m^2 means that each side is 0.71 m.

Table 2. The input data for the simulations of the scale model.

f [Hz]	250	500	1 k	2 k	4 k	8 k	16 k
α_{av}	0.032	0.033	0.034	0.038	0.038	0.035	0.035
α_{ceil}	0.826	0.832	0.876	0.945	0.969	0.965	0.972
α_{sin}	0.100	0.217	0.179	0.076	0.049	0.096	0.071
s_w	0.005	0.03	0.03	0.04	0.04	0.04	0.04
s_c	0.01	0.01	0.01	0.01	0.01	0.01	0.01
s_{sin}	0.038	0.076	0.167	0.404	0.509	0.592	0.633
$s_{sin,O}$	0.02	0.15	0.35	0.45	0.5	0.53	0.6
d_{LS}	1	1	0.5	0	0	0	0

To investigate whether it is sufficient for the sinusoidal diffuser to use a standard frequency dependence as is done in ODEON, a PARISM simulation is done with scattering coefficients that were estimated from the 0.25 curve in the manual. These scattering coefficients can be seen in Table 2 as $s_{sin,O}$. The frequency average of the scattering coefficient is 0.35, and a PARISM simulation is furthermore carried out with this value for all frequencies to test the influence of disregarding the frequency dependence.

Because it is not at present possible to include a directivity pattern in PARISM, the directivity of the loudspeaker was considered by applying a frequency dependent factor to the first reflections of the three surfaces behind the source. From the directivity patterns, the factor in terms of energy was set as can be seen in Table 2 denoted d_{LS}.

5.2.2 Method of the ODEON simulations

For the sinusoidal diffuser the average scattering coefficient of the 500 Hz and 1 kHz octave bands is 0.12, but when looking at the frequency curves given in the manual it seems that the curve for a scattering coefficient of around 0.1 will not be steep enough to give a high enough scattering coefficient at higher frequencies. The curve of a mid-frequency scattering coefficient of 0.25 seemed to be a better fit as it is just over 0.5 at 8 kHz. This was therefore the chosen value. The scattering coefficients of the wall and floor were set to 0.01 and those of the walls were set to 0.04.

Because it is possible in ODEON to include a full 3-dimensional directivity pattern, this was done for the loudspeaker. It was assumed that the directivity of the loudspeaker is rotationally symmetric around its normal axis.

5.3 Results

The results of the measurements and the simulations are regarded in terms of the room acoustical parameters reverberation time (T_{30}) and early decay time (EDT).

5.3.1 The furnished room

The results of the first example are shown in Fig. 6, where it is seen that neither PARISM nor ODEON perfectly match the measurements in terms of frequency dependence, differences between the reverberation times and the early decay time and the influence of the furniture.

The difference between V_1 and V_2 is larger for the reverberation times than the early decay time. When comparing the simulation results with V_1 and V_2 to the simulations without a scattering volume, it is seen that V_1 does not influence the reverberation time much, indicating that only the early part of the decay is affected by V_1. Because the room has an absorbing ceiling, the reflections that make up the late part of the decay are the chains of reflections by the walls and not by the floor and the ceiling. If the height of the scattering volume is below the height of the source and the receiver, these reflections will for the image source method not have been influenced by the scattering volume. When the height is above, they will however be influenced. In the measurements, both the source and the receiver were above the tables and chairs, but the reverberation time and thus the late part of the decay is clearly influenced by the objects. It is an interesting observation that it is necessary to increase the height of the scattering volume in the simulations to see the same effect.

It is furthermore seen that ODEON tends to underestimate the reverberation time and even more the early decay time. It furthermore seems that ODEON underestimates the frequency dependence of the parameters, which can be due to the neglect of phase information and thus the exclusion of room modes.

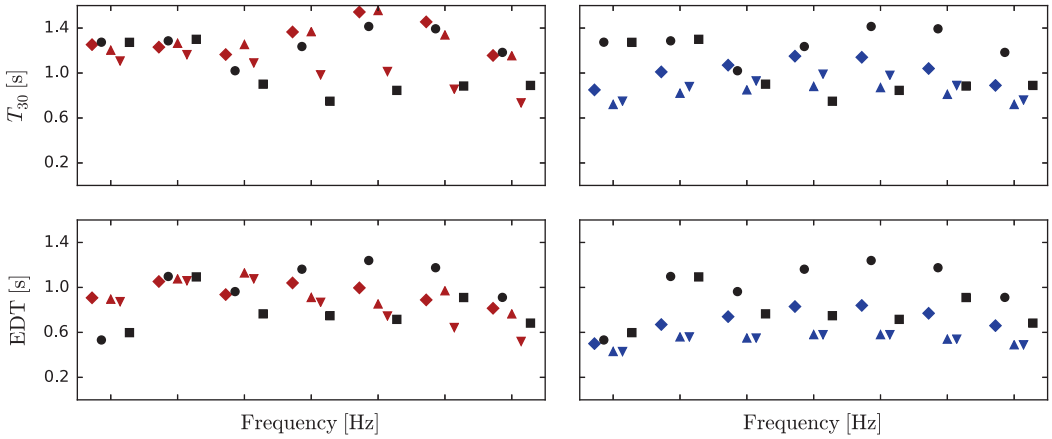

Figure 6: **Left: PARISM and measurements.** *Red diamond:* PARISM without scattering volume. *Black circle:* Measurement in empty room. *Red upward pointing triangle:* PARISM with scattering volume V_1. *Red downward pointing triangle:* PARISM with scattering volume V_2. *Black square:* Measurement in furnished room. **Right: ODEON and measurements.** *Blue diamond:* ODEON without scattering box. *Black circle:* Measurement in empty room. *Blue upward pointing triangle:* ODEON with impenetrable box. *Blue downward pointing triangle:* ODEON with semi-transparent box. *Black square:* Measurement in furnished room.

The ODEON simulations show that making the surfaces of the box semi-transparent decreases the reverberation times and the early decay time very slightly. The decrease can be unexpected as the acoustic volume should be largest with the penetrable box, thus giving a slower decay. But an explanation can be that a semi-transparent surface is semi-transparent from both sides, which means that if a ray enters the box it is reflected from the floor and can then be reflected by one of the sides of the box with the probability of the transparency. If it is reflected by a box surface, the absorption coefficient of box surfaces will be used. Some rays will therefore be trapped and reflected several times in the box, and the energy of the ray will have decreased when it leaves the box. The semi-transparent box can therefore function as added absorption, especially if the absorption coefficients of the box surfaces are high compared to the other surfaces. A box enclosing scattering objects should therefore only be semi-transparent if the objects are expected to trap sound in such a way. This corresponds well with the recommendation of the ODOEN manual to use semi-transparent surfaces when several surfaces are modeled by a single surface.

5.3.2 The scale model with sinusoidal diffuser

The results of the measurements and the simulations of the scale model are shown in Fig. 7, where it is seen that the orientation of the diffuser does have an influence on the results. This indicates that the random incidence scattering coefficient that is measured under assumed diffuse field conditions can be be insufficient to describe the influence of the diffuser on a non-diffuse sound field. It could therefore be interesting to be able to include an angle-dependent scattering coefficient in the simulations.

Both PARISM and ODEON seem to underestimate the influence of the diffuser, especially when regarding the reverberation times indicating that the later part of the decay is not sufficiently influenced. An interesting observation is that the T_{30}-values are even increased by the introduction of the diffuser in the ODEON simulations. From the ODEON simulations, it is again observed that the frequency dependence of the reverberation times and the early decay times is underestimated.

Looking at the PARISM results with different frequency dependencies of the scattering coefficient of the sinusoidal diffuser, it must be noted that the predefined dependency of ODEON seems to be adequate for this diffuser. It must also noted that a decrease in the scattering coefficient towards lower frequencies is important in the simulations as shown by the simulations with a frequency-independent scattering coefficient.

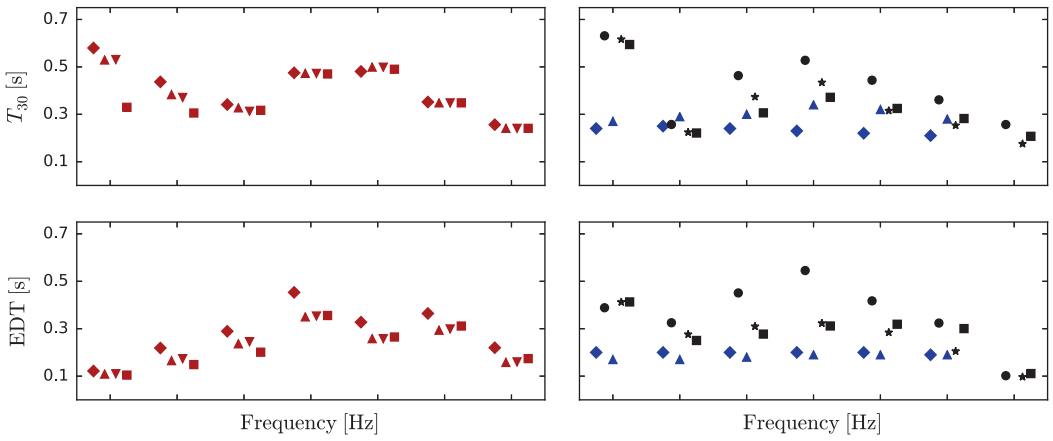

Figure 7: **Left: PARISM.** *Red diamond:* PARISM without scattering. *Red upward pointing triangle:* PARISM with sinusoidal diffuser. *Red downward pointing triangle:* PARISM with sinusoidal diffuser with $s_{sin,O}$. *Red square:* PARISM with sinusoidal diffuser without frequency dependence. **Right: ODEON and measurements.** *Blue diamond:* ODEON without scattering. *Black circle:* Measurement in empty room. *Blue upward pointing triangle:* ODEON with sinusoidal diffuser. *Black star:* Measurement with sinusoidal diffuser parallel to horizontal. *Black square:* Measurement with sinusoidal diffuser parallel to vertical.

6. CONCLUSION

It has been shown how it is possible to determine the attenuation by a scattering volume of a known bulk scattering coefficient and at the same time account for the scattered energy, such that no energy is lost. The same was shown when a reflecting surfaces is present close to the scattering volume.

The method of scattering from a volume has been implemented in the room acoustical model PARISM and results were obtained that corresponded quite well with measurement results, though it was observed that the height of the scattering volume had to be increased compared to the height of the actual objects to obtain an influence on the late part of the decay as was seen in the measurements. The volume scattering method is at a very early stage of development and though it shows some promising results, it is clear that more investigations are needed of its influence in room acoustic simulations.

It was shown that the frequency dependence of the scattering from the sinusoidal diffuser investigated in the present example is adequately described by the predefined pattern that is given in the ODEON manual. It was however seen that a completely flat frequency dependence is not sufficient. From the measurements, it was seen that the orientation of the diffuser had an influence on the results, which indicates that the diffuser is insufficiently described by the random incidence scattering coefficient, and it could therefore improve the precision of simulations to use an angle-dependent scattering coefficient.

ACKNOWLEDGMENTS

The authors are very grateful for the discussions with Peter Svensson about scattering from objects and the determination of bulk scattering coefficient from edge diffraction. A thank you is also given to Alejandro Gonzalez Pacheco and Japhet Kabura for the work of the measurements used for comparisons.

REFERENCES

[1] T. J. Cox, B.-I. L. Dalenbäck, P. D'Antonio, J. J. Embrechts, J. Y. Jeon, E. Mommertz, and M. Vorländer. A tutorial on scattering and diffusion coefficients for room acoustic surfaces. *Acta Acust. united Ac.*, 95:1–15, 2006.

[2] B.-I. Dalenbäck, M. Kleiner, and P. Svensson. A macroscopic view of diffuse reflection. *J. Audio Eng. Soc.*, 42:793–807, 1994.

[3] M. Hodgson. Evidence of diffuse surface reflections in rooms. *J. Acoust. Soc. Am.*, 89:765–771, 1991.

[4] C. Lynge, G. Koutsouris, and J. Gil. *ODEON manual version 13*. ODEON, Kgs. Lyngby, 2016.

[5] E. A. Lindqvist. Sound attenuation in large factory spaces. *Acta Acust. united Ac.*, 50:313–328, 1982.

[6] U. J. Kurze. Scattering of sound in industrial spaces. *J. Sound Vib.*, 98:349–364, 1985.

[7] M. Hodgson. On the accuracy of models for predicting sound propagation in fitted rooms. *J. Acoust. Soc. Am.*, 88:871–878, 1990.

[8] A. M. Ondet and J. L. Barbry. Sound propagation in fitted rooms - comparison of different models. *J. Sound Vib.*, 125:137–149, 1988.

[9] A. M. Ondet and J. L. Barbry. Note in connection with a comparison of different models for predicting sound levels in fitted industrial rooms. *J. Sound Vib.*, 143:343–350, 1990.

[10] S. M. Dance and B. M. Shield. The complete image-source method for prediction of sound distribution in non-diffuse enclosed spaces. *J. Sound Vib.*, 201:473–489, 1997.

[11] C. L. Morfey. *Dictionary of Acoustics*. Academic Press, London, 2001.

[12] G. Marbjerg, J. Brunskog, C.-H. Jeong, and E. Nilsson. Description and validation of a combined phased acoustical radiosity and image source model for predicting sound fields in rooms. *J. Acoust. Soc. Am.*, 138:1457–1468, 2015.

[13] G. I. Koutsouris, J. Brunskog, C.-H. Jeong, and F. Jacobsen. Combination of acoustical radiosity and the image source method. *J. Acoust. Soc. Am.*, 133:3963–3974, 2013.

[14] G. A. Daigle. Diffraction of sound by noise barrier in the presence of atmospheric turbulence. *J. Acoust. Soc. Am.*, 71:847–854, 1982.

[15] J. Forssén, M. Hornikx, D. Botteldooren, W. Wei, T. Van Renterghem, and M. Ögren. A model of sound scattering by atmospheric turbulence for use in noise mapping calculations. *Acta Acust. united Ac.*, 100:810–815, 2014.

[16] G. Marbjerg, J. Brunskog, C.-H. Jeong, and E. Nilsson. A method of modeling continuous volume scattering from objects for geometrical room acoustic simulations, 2016.

[17] E.-M. Nosal, M. Hodgson, and I. Ashdown. Improved algoritms and methods for room sound-field prediction by acoustical radiosity in arbitrary polyhedral rooms. *J. Acoust. Soc. Am.*, 116:970–980, 2004.

[18] X. Zeng, C. L. Christensen, and J. H. Rindel. Practical methods to define scattering coefficients in a room acoustics computer model. *Appl. Acoust.*, 67:771–786, 2006.

[19] Y. Miki. Acoustical properties of porous materials - modifications of delany-bazley. *J. Acoust. Soc. Jpn.*, 11:19–24, 1990.

[20] G. Marbjerg, P. Svensson, J. Brunskog, C.-H. Jeong, and E. Nilsson. Determining a random incidence scattering cross section from edge diffraction of rectangular objects, 2016.

[21] U. P. Svensson, R. I. Fred, and J. Vanderkooy. An analytic secondary source model of edge diffraction impulse responses. *J. Acoust. Soc. Am.*, 105:2331–2344, 1999.

[22] U. P. Svensson. Edge diffraction toolbox. http://www.iet.ntnu.no/~svensson/software/index.html, 2015.

[23] L. L. Beranek and T. Hidaka. Sound absorption in concert halls by seats, occupied and unoccupied, and by the hall's interior surfaces. *J. Acoust. Soc. Am.*, 104:3169–3177, 1998.

[24] ISO standard 17497-1 - sound-scattering properties of surfaces - part 1: Measurement of the random-incidence scattering coefficient in a reverberation room. *International Organization for Standardization, Geneva, Switzerland*, 2004.

[25] ISO standard 354 - measurement of sound absorption in a reverberation room. *International Organization for Standardization, Geneva, Switzerland*, 2003.